Control of (1+1+1′)-photon dissociation dynamics in the NaH molecule using three delayed ultrashort pulses

Anindita Bhattacharjee* and Krishna Rai Dastidar†
Department of Spectroscopy, Indian Association for the Cultivation of Science, Kolkata 700032, India
(Received 1 September 2004; published 29 August 2005)

We have calculated (1+1+1′)-photon dissociation cross section of the NaH molecule from $v''=0$ level of the ground $X\ ^1\Sigma^+$ state to the repulsive $B^1\Pi$ state via the bound $A\ ^1\Sigma^+$ state by using three delayed ultrashort pulses. Two delayed 4 femtosecond pulses have been used for the first step transition to design interfering wave packets on the intermediate $A\ ^1\Sigma^+$ state and the third delayed ultrashort pulse (either δ-function or 4 femtosecond) excites these wave packets to the dissociating state. We have shown that control over dissociation dynamics can be achieved by controlling delay between three pulses, the pulse durations, and the carrier frequencies. We have considered two values of delay between the first two 4 femtosecond pulses for which it is possible to inhibit and enhance the deexcitation channel to the ground state and hence for these two delays the maximum of the cross section in the dissociation spectrum can be enhanced or diminished respectively for the δ-function transition to the dissociating state by the third ultrashort pulse. The dissociation spectrum also depends on the delay of the third pulse. The dependence of the dissociation cross section on the delays of pulses and on the carrier frequency of the third pulse has been demonstrated for two step dissociating transition by three delayed 4 femtosecond pulses of Gaussian shape. It has been suggested that the oscillation of dissociation cross section with time delay of the third pulse can be realized as time dependent quantum gates and the nature of quantum gates can be controlled by choosing pulses of different shape, duration, and photon energy (or carrier frequency) as well as delay between the pulses. This aspect of realization and precise control of time dependent quantum gate in light molecules by using three ultrashort pulses (4 femtosecond) has not been explored before.

DOI: 10.1103/PhysRevA.72.023419 PACS number(s): 42.50.Gy, 42.50.Hz

I. INTRODUCTION

For the past few decades, there have been considerable efforts to achieve control over chemical reactions [1–22]. With the advent of ultrashort laser pulses, scientists have been able to understand and control the real time dynamics of chemical reactions. Atomic or molecular processes can be controlled in various ways [1–4]. Brumer and Shapiro [2] have shown that control over products can be achieved by utilizing quantum coherence and interference between different channels. Multiple laser fields are employed whose relative intensities and phases are varied to obtain control over products. The optimal control technique [3] aims at designing a set of pulses that work cooperatively to force the system to attain a particular desired state. The third way of achieving control is by using short duration broadband pulses to generate a wave packet and then by controlling the duration of wave packet propagation on the excited state as initially shown by Tannor and Rice [4]. Since then, there have been numerous experimental and theoretical studies using short pulses to generate a wave packet on the excited surface and subsequently to probe the wave packet by another time delayed pulse. At time scales smaller than the atomic and molecular time scales, the wave packets on the excited state are localized and hence their motion can be studied and controlled [5–12,15–22]. Wave packet control has found applicability in various fields like isotope separation [6], control of vibrational motion [7] etc. The motion of the wave packet can be probed by using a second pulse by various means. Dantus *et al.* [5] studied the wave packet motion on a repulsive surface in the molecule ICN by exciting the moving wave packet on another repulsive state from where the fluorescence signal was observed. The motion of a vibrational wave packet in Na_2 was studied by Gerber and co-workers [8]. The moving wave packet was studied by multiphoton excitation to an ionizing state where the transient ionization spectra were measured. Using a three-photon excitation scheme in Li_2, Leone and co-workers [9] studied the motion of a three-dimensional wave packet via ionization and observed both vibrational and rotational recurrences. In theoretical studies on atomic Rydberg [10] and molecular vibrational wave packets [11] fluorescence/Raman spectrum was calculated. It has been found that dissociating wave packets can be completely characterized by experimental determination of kinetic energy distribution and measurement of fluorescence signal from one of the fragments [12]. Reaction dynamics or yield in molecular systems can also be controlled by controlling the phase of the generated short pulse [13–16]. As shown by Chelkowski *et al.* [13], using a chirped ultrashort pulse, molecular dissociation probability can be largely enhanced. Recently it was shown that by appropriate pulse shaping resonant multiphoton transitions can be significantly enhanced [14]. Very recently it was shown [15] that by using trains of phase locked pulses, population in specific rotational states can be controlled in molecular Rydberg wave packets. Control of wave packet dynamics by

*Email address: anny_b_2000@yahoo.com
†Email address: spkrd@mahendra.iacs.res.in

varying the relative phases of the different rovibrational wave packet components using shaped femtosecond pulses was shown by Uberna *et al.* [16]. By optimizing the phases of the wave packet components, the three-dimensional wave packet could be partially localized in specific regions of space.

Recently, much attention is being given to the study of interference of wave packets on atomic or molecular potential surfaces [17–22]. Noel and Stroud [18] studied Young's double slit interference pattern within an atom by using phase-coherent pulses to excite wave packets and their interference was probed by a third pulse. Temporal coherent control of the ionization probability was achieved by ionizing two interfering wave packets in Cs_2 dimer [20]. It was recently shown that interfering wave packets in a dissociating molecule can be imaged and controlled by phase difference between two dissociating pulses [21]. Interfering nuclear wave packet on a molecular surface produced by two phase delayed femtosecond pulses was recently studied by Ohmori *et al.* [22] by probing it by a nanosecond pulse. It was shown that relative population in the three vibrational levels which constitute the wave packet can be arbitrarily prepared only by controlling the delay time. In this work we have shown that the dissociation cross section upon excitation of the interfering wave packets on the bound state can be controlled by controlling the delays between consecutive pulses. The delay between the first two pulses allows preparation of the wave packet on the bound state and hence controls its shape and magnitude as desired, whereas the delay between the second and the third pulse allows the wave packet to oscillate on the bound state and further change its shape and location. Thus control over the $(1+1+1')$-photon dissociation cross section can be achieved by controlling these two delays.

In an earlier work, we have shown that $(1+1')$-photon dissociation cross section oscillates with time delay between two ultrashort pulses. At a particular frequency of the second pulse the oscillation in dissociation cross section can be controlled by controlling the delay between pulses [23] and this oscillation in the cross section can be used as a time-dependent quantum gate. In the present work, a wave packet has been designed on the excited $A\ ^1\Sigma^+$ state using two identical delayed pulses. The designed wave packet is produced from the interference of the two wave packets excited by first two pulses and its shape and positions are dependent on the delay time between two pulses. This interfering wave packet is allowed to propagate freely on the bound state surface until it is excited to the repulsive state by the third pulse. Therefore the wave packet also changes its shape and position differently for different delays between the second and the third pulse before excitation to the dissociating repulsive state. Thus, effectively a wave packet can be designed on the repulsive state leading to dissociation as desired. Hence the fine-tuning of dissociation can be achieved by tuning the two delays between three pulses. At a particular frequency of the third pulse, it has been shown that the dissociation cross section oscillates with the time delay between the second and the third pulse and the zeros and the maxima of the cross section appear at different time delays for different designed (by the first two pulses) wave packets. This difference in the position of zeros and maxima of the cross section is due to the difference in the shape and location of the wave packets on the bound excited state. Thus this oscillation in dissociation cross section can be realized as quantum gate and one can control this time dependent quantum gate by exciting different designed wave packets. Earlier, Barenco *et al.* [24] have used Ramsey interferometry with Rydberg wave packets in atoms to construct quantum logic gates. Here we have shown that by designing and controlling molecular wave packets on the bound intermediate and repulsive dissociating state one can control the time dependent quantum gate in $(1+1+1')$-photon dissociation by three ultrashort pulses. In $(1+1')$-photon dissociation [23] the designing of wave packet on the bound state is controlled only by the delay between pulses during which the wave packet propagates freely on the bound state to change its shape and position. But in the present case zeros and maxima of oscillating dissociation cross section can be further controlled by changing delay between the first two pulses thus leading to further control over the nature of quantum gates. We have used 4 femtosecond (4 fs) Gaussian pulses for the first two excitations. For the third excitation, two kinds of pulses, viz., a δ-function pulse and a 4 fs Gaussian pulse were considered. It was shown earlier [23] that excitation by very short pulses (1 fs) can be approximated as δ-function excitation. Using a 4 fs Gaussian pulse for the third excitation, it has been found that the position of zeroes and the maxima and also the nature of oscillation are different from those for the δ-function excitation. We have shown here that for light molecules one has to choose ultrashort pulses (4 fs) to get precise control over the dissociation process and hence on the quantum gate, since the wave packets in light molecules are delocalized within a very short time. This aspect of controlling time dependent quantum gate by properly choosing the duration, shape, frequency and the delay between the pulses, has not been addressed in detail before.

It has also been shown that one can design interfering wave packets on the intermediate state by properly choosing the delay between first two pulses such that the dissociation can be enhanced and diminished and hence the de-excitation to the lowest vibrational level of the ground state can be inhibited and enhanced respectively. Therefore one can selectively deexcite the molecule to a single vibrational level of the ground state (by properly choosing the delay between the first two 4 fs pulses) although the ultrashort pulse has a very broad bandwidth which can cause deexcitation to a large number of vibrational levels. This feature of dependence of selectivity in deexcitation to a single vibrational level of the ground state on the delay between the ultrashort pulses (the bandwidth of which covers at least five vibrational levels of the ground state) has not been demonstrated before. Earlier, it was only shown that with pulses of narrow bandwidth the molecule can be deexcited to a bundle of three levels [25].

In this work, we have calculated the $(1+1+1')$-photon dissociation spectrum by solving the one-dimensional time dependent Schrödinger equation on the two excited state surfaces for which time dependent Fourier grid method [26] has been used. This method has been widely used to calculate

photodissociation spectra [23,27,28] by single photon. To compute the photoexcitation and dissociation spectra of the molecule, Heller's model [29] was considered. This method enables computation of the whole spectrum in a single calculation when pulses of infinitely short duration (e.g., δ function) are considered. For pulses of longer duration, a modified theory [30] has been used.

The recent developments in ultrashort pulses [31] have encouraged us to consider pulses as short as 4 fs and the δ-function pulses. Attosecond pulses are recently being used to study the dynamics of electrons in atoms [32] and controlling various related processes in atoms [33] and molecules [34].

II. THEORY

We have used the time dependent Fourier grid method of Balint-Kurti [26] which combines the Fourier grid Hamiltonian method [35] along with Heller's model of photodissociation and Chebyshev time propagation scheme [36]. The details of this method can be found in the literature [26,28]. In this model, an initial wave packet $\phi(t=0)$ is constructed from the product of the ground state wave function $\psi(E_i)$ and the electronic dipole transition moment $\mu(R)$ for that transition:

$$|\phi(t=0)\rangle = \mu(R)|\psi(E_i)\rangle. \tag{1}$$

The ground vibrational wave function is obtained by using the Fourier grid Hamiltonian method described in [23,26,28,35] for which the spatial 1-dimensional grid is set up on the internuclear axis.

In the Fourier grid Hamiltonian method, the potential energy operator is treated in the coordinate representation and the kinetic energy operator is treated in the momentum representation where they are respectively diagonal. Fourier transform is used to switch between the two representations. The continuous range of coordinate and momentum values are replaced by grids in coordinate and momentum space. The wave function is represented as a vector in the coordinate space whose components are the values of the function at the grid points. The Hamiltonian matrix is calculated from the potential energy and kinetic energy values at the grid points. By diagonalizing the Hamiltonian matrix one can obtain the bound state eigenvalues and eigenvectors (amplitudes of eigenfunction of the Schrödinger equation at the grid points).

The initial wave packet $|\phi(t=0)\rangle$ is propagated on the excited state potential energy surface. Time developed wave packets are calculated by Chebyshev scheme [36]. The entire time interval is divided into small time steps and at each time step the wave packet is calculated and hence the autocorrelation function, i.e., the overlap of the initial wave packet with the wave packet at a later time t, is obtained as

$$F(t) = \langle \phi(t=0)|\phi(t)\rangle. \tag{2}$$

Fourier transform of the autocorrelation function gives the required absorption spectrum (neglecting the effect of rotation).

$$\sigma(\nu) = \frac{\pi\nu}{3c\epsilon_0\hbar}\int_{t=-\infty}^{\infty} e^{iEt/\hbar}F(t)dt, \tag{3}$$

where c is the velocity of light, ϵ_0 is the permittivity of free space, and $E=E_i+h\nu$, E_i being the energy of the initial vibrational state. While computing the cross section for $\Sigma \rightarrow \Pi$ transition, the degeneracy factor should be included in Eq. (3).

This method for studying single photon absorption and for δ-function transition has been extended to study a two-photon process [23] using pulses of finite width. It can be further extended to study the (1+1+1′)-photon dissociation spectrum. The time-dependent wave packet for excitation by a pulse of finite width has been obtained by Lee and Heller [30]. Time dependent wave packet can also be found in the work of Schinke [37] and Pollard *et al.* [38]. The wave packet amplitude on the excited surface "e" at time $t=T$ and at internuclear separation R is

$$(i\hbar)\chi_{e1}(R,T) = \int_0^T dt_1 e^{-iH_e(T-t_1)/\hbar} \times [D_{eg}(R)\epsilon(t_1)]e^{-iH_g t_1/\hbar}\chi_{gv}(R,0), \tag{4}$$

where $\chi_{gv}(R,0)$ is the eigenfunction of the vibrational level "v" of the ground state g at time $t=0$. H_g and H_e are the total Hamiltonian for the ground state "g" and the excited state "e," respectively. D_{ge} is the electronic dipole transition moment for transition from the ground state "g" to the state "e."

By the first pulse, the molecule is excited from the ground vibronic state to the intermediate $A\ ^1\Sigma^+$ state where the wave packet is given by Eq. (4). The radiation field is switched off after a time T (duration of the first pulse) and the wave packet is allowed to propagate freely on the $A\ ^1\Sigma^+$ state for a time interval τ_1 (delay between the first two excitation pulses). The second pulse is switched on at time $T+\tau_1$, which excites another wave packet $\chi_{e2}(R,T+\tau_1+T')$ on the $A\ ^1\Sigma^+$ state surface of the same form as in Eq. (4), with T being replaced by T' which is the duration of the second pulse and $\chi_{gv}(R,0)$ being replaced by $\chi_{gv}(R,T+\tau_1)$. The first wave packet has evolved for a time τ_1+T'. The resultant wave packet on the $A\ ^1\Sigma^+$ state surface at time $T+\tau_1+T'$ is the sum of the two wave packets and is given by

$$\chi_e(R,T+\tau_1+T') = \chi_{e1}(R,T+\tau_1+T') + \chi_{e2}(R,T+\tau_1+T') \tag{5}$$

and it is allowed to propagate for time τ_2. The third pulse of duration T'' is switched on at time $T+\tau_1+T'+\tau_2$ which excites the propagated wave packet on the second excited surface "f." The wave packet amplitude on the second excited surface f is

$$(i\hbar)\chi_f(R,T+\tau_1+T'+\tau_2+T'') = \int_{T+\tau_1+T'+\tau_2}^{T''} dt_2 e^{-iH_f(T''-t_2)/\hbar}[D_{fe}(R)\epsilon(t_2)]e^{-iH_e t_2/\hbar} \times \chi_e(R,T+\tau_1+T'+\tau_2), \tag{6}$$

where $\chi_e(R,T+\tau_1+T'+\tau_2)$ is the propagated wave packet on

state "e." D_{ef} is the electronic dipole transition moment for second step transition and H_f is the total Hamiltonian of the state "f." Here, the electric field is on for the duration $T+\tau_1+T'+\tau_2$ to T''. The wave packets have been calculated at each spatial grid point. $\epsilon(t_i)$ in Eqs. (4) and (6) is the electric field at time t_i given by

$$\epsilon(t_i) = g(t_i)\exp[i(\omega t_i + \theta_i)], \tag{7}$$

where $g(t_i)$ is the temporal profile of the pulse, θ_i is the phase, and ω is the carrier frequency. By propagating the wave packet χ_f on the dissociative f state we can obtain the autocorrelation function at different time (by integrating over the space coordinate) defined in Eq. (2). Fourier transform of the autocorrelation function [Eq. (3)] gives the dissociation cross section at the carrier frequency.

The phase θ_i in Eq. (7) for the three pulses has been chosen to be zero. For long pulses ($\sim$100 fs), it has been shown that the relative phase of the pulses can be neglected when there is a single channel for transition to the final state (see Sec. IV B of Ref. [16]). However, for ultrashort pulses like that considered here, the carrier-envelope phase, which is the relative phase between the maximum of the pulse envelope and the nearest maximum of the carrier wave, becomes crucial [39–41]. First, this quantity is highly sensitive to fluctuations in pulse intensity, etc. Second, it was shown in different experimental and theoretical studies that phenomena like high harmonic generation [42], atomic photoionization [43] and above threshold ionization [44] are dependent on the absolute phase. The phase stabilization of ultrashort pulses was recently achieved [33]. It was shown by Brabec and Krausz (p. 561 of Ref. [41]) that for Gaussian pulse, the use of cycle-averaged intensity from the envelope down to pulse duration approaching the carrier oscillation cycle is justified and the description of pulsed electromagnetic field in terms of carrier and envelope is legitimate for pulse duration greater than carrier oscillation period. The 4 fs pulses considered in this study are 3-cycle pulses for the first two transitions whereas for the third transition the pulse (4 fs) is nearly one-cycle. Thus these pulses can be considered stable with fluctuations in intensity. However, the effect of overall carrier-envelope phase should be significant. It was shown by Chelkowski and Bandrauk [43] that the dependence of atomic photoionization yields was strong for pulses comprising less than 15 cycles which leads to directional photoelectron asymmetries along the laser polarization vector. Hence, the overall carrier phase of the pulses can influence results in our calculation and the study on the effect of carrier phase on dissociation and deexcitation is warranted.

To obtain the cross section for deexcitation of the propagating wave packet $\chi_{e1}(R, T+\tau_1)$ by the second pulse after a delay time τ_1, we have calculated the wave packet generated on the ground state at a particular carrier frequency of the second pulse (4 fs Gaussian) which is again propagated on the ground state surface for a long time. The autocorrelation function at different times during the propagation is Fourier transformed to give the total deexcitation cross section at that carrier frequency.

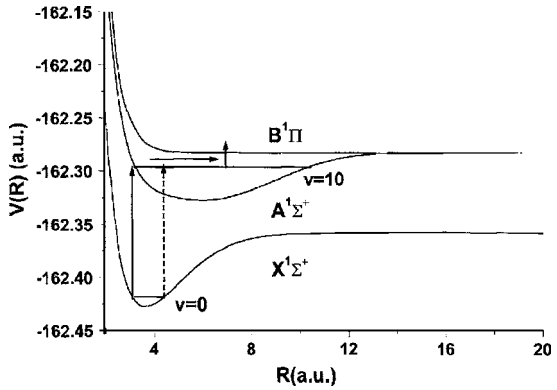

FIG. 1. Potential energy curves for the $X\ ^1\Sigma^+$, $A\ ^1\Sigma^+$, and $B\ ^1\Pi$ electronic states of the NaH molecule.

III. CALCULATIONS

We have considered excitation from $v''=0$ level of the ground electronic state of NaH. *Ab initio* potential energy curves for the electronic states $X\ ^1\Sigma^+$, $A\ ^1\Sigma^+$, and $B\ ^1\Pi$ states and also the dipole transition moments for the $X\ ^1\Sigma^+ \rightarrow A\ ^1\Sigma^+$ and $A\ ^1\Sigma^+ \rightarrow B\ ^1\Pi$ transitions have been obtained from the literature [45]. The potential energy curves for the ground state ($X\ ^1\Sigma^+$) and the two excited states ($A\ ^1\Sigma^+$ and $B\ ^1\Pi$) are shown in Fig. 1. We have considered a one-dimensional grid of length 19.8 a.u. and 1024 number of grid points. An imaginary damping potential was added in the asymptotic region to stop the wave packet from getting reflected at the edge of the grid. The time step for propagation was 5 a.u. for both the $X\ ^1\Sigma^+ \rightarrow A\ ^1\Sigma^+$ and $A\ ^1\Sigma^+ \rightarrow B\ ^1\Pi$ transitions. The accuracy of the calculation is determined by the convergence of energy and autocorrelation function. For the bound-bound calculation, the convergence of energy is within 0.03 percent. Convergence of energy for the bound-continuum calculations are within 0.01 and 1 percent. The ratio of final to initial autocorrelation function is within 1.5×10^{-5} for these calculations. Calculations have been done with δ-function and Gaussian pulses. The delta function pulse is considered of the form

$$g(t) = \delta(t). \tag{8}$$

For the Gaussian pulses, a normalized profile of the form

$$g(t) = \frac{1}{\sqrt{2\pi}\sigma} e^{-t^2/2\sigma^2} \tag{9}$$

was considered. The value of σ varied with the width of the pulse. Gaussian pulses of width (FWHM) 4 fs have been considered for the two excitations from ground state to the intermediate state. The lower and upper limit of the time integration in Eqs. (4) and (6) are so chosen that the value of the temporal profile reduces to 10^{-4} times the peak value on both sides of the center of the Gaussian profile.

Two sets of excitation schemes have been considered for the third excitation to the dissociative state: (i) δ-function excitation, where $g(t)$ is considered to be a δ function; (ii) excitation by a 4 fs Gaussian pulse. For the δ-function transition, delay time τ_2 have been considered in steps of

250 a.u. In the calculations using Gaussian shaped pulses, we have considered delay times in steps of 500 a.u. The pump laser photon energy has been considered to be 25 310 cm^{-1} (395.57 nm) resonant with the $v'=10$ of the intermediate state and has been used as the carrier frequency for the first step $X\ ^1\Sigma^+ \rightarrow A\ ^1\Sigma^+$ transition. The bandwidth of the laser covers a number of vibrational levels on both sides of the $v'=10$ level depending upon its duration and temporal profile. A 4 fs Gaussian pulse has a bandwidth [full width at half maximum (FWHM)] of 3666 cm^{-1} that covers the vibrational levels $v'=6$ to $v'=14$ of the intermediate state. The probe laser was tuned at different frequencies and dissociation cross section at those carrier frequencies were obtained. For the calculation of the deexcitation cross sections to the different vibrational levels ($v''=0-2$) of the ground state, we have considered three carrier frequencies which match with the transitions from the $v'=10$ level of $A\ ^1\Sigma^+$ state to the $v''=0-2$ levels of $X\ ^1\Sigma^+$ state. To show the prominence of peaks at these three resonant frequencies, we have repeated the calculation with carrier frequencies between these three matching frequencies.

IV. RESULTS AND DISCUSSIONS

The first pulse of FWHM 4 fs and of Gaussian shape excites a wave packet from the $v''=0$ level of the ground $X\ ^1\Sigma^+$ state to the $A\ ^1\Sigma^+$ state. The carrier frequency of the pulse is 25 310 cm^{-1}, which corresponds to a resonant excitation to the $v'=10$ level of the excited state. Due to the finite bandwidth of the pulse, vibrational levels $v'=6-14$ of the $A\ ^1\Sigma^+$ state are excited. The wave packet is allowed to propagate on the bound surface. It oscillates between inner and outer turning points in the potential well attaining different shapes and locations with time. After a delay, a second pulse identical in shape, width, and carrier frequency and in phase with the first pulse pumps up another wave packet on the $A\ ^1\Sigma^+$ state surface, which interferes with the first wave packet propagating on this surface. At different delays τ_1, the shapes and locations of the first and second wave packets are different and hence the resultant interfering wave packet on the $A\ ^1\Sigma^+$ state surface changes with τ_1. At delay times $\tau_1=1000$ a.u. ~ 24 fs and $\tau_1=2000$ a.u. ~ 48 fs, the wave packet on the $A\ ^1\Sigma^+$ state denoted by wp1 and wp2 are shown in the inset of Fig. 2. The square of the complex wave packet is plotted against the internuclear separation. The wave packet wp1 at $\tau_1=1000$ a.u. is localized around 7 a.u. on the internuclear axis, whereas at $\tau_1=2000$ a.u. the wave packet wp2 is concentrated at two points, around 3.5 a.u. and around 6 a.u. As the wave packet wp1 is excited around $R=7$ a.u. where the dipole transition moment for $X\ ^1\Sigma^+ \rightarrow A\ ^1\Sigma^+$ transition $\mu_{AX}(R)$ is the strongest, its magnitude is high. $\mu_{AX}(R)$ is nearly halved at $R=3.5$ a.u., hence the magnitude of the wave packet wp2 is small. Besides the interference effects in these two wave packets are prominent. When the wave packet on the $A\ ^1\Sigma^+$ state is further excited to the repulsive $B\ ^1\Pi$ state by a third pulse, the wave packet slides down the repulsive state and the molecule dissociates. The photodissociation cross section for δ-function excitation of the wave packets wp1 and wp2 are shown in Fig. 2 (for $\tau_2=0$) by solid and dashed curves, respectively. The cross section is higher for wp1 ($\tau_1=1000$ a.u.) than that for wp2 ($\tau_1=2000$ a.u.), as the magnitude of wave packet wp1 is larger than wp2. The branch of the wave packet (wp2) around $R=3.5$ a.u. upon excitation to the repulsive state reaches at a point where the potential energy curve is steep and covers a wide range of energy to reach the asymptotic region, hence the dissociation spectrum is broader. It should be noted that if we allow the wave packets wp1 and wp2 to freely propagate for a time period before exciting it to the dissociative surface, the shape and magnitude of both the wave packets on the intermediate state surface will change. Accordingly the magnitude and shape of the final dissociation spectrum for both the wave packets will be different from that presented in Fig. 2.

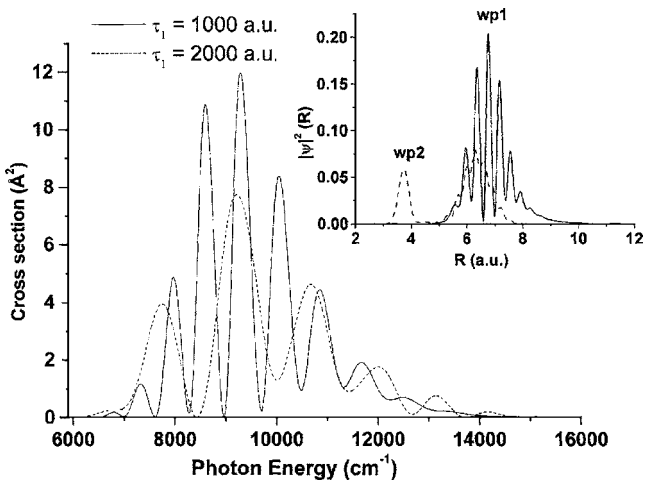

FIG. 2. Photodissociation cross section at different photon energies for δ-function excitation of two wave packets wp1 and wp2 on the $A\ ^1\Sigma^+$ state surface to the dissociative $B\ ^1\Pi$ state surface of NaH at a delay $\tau_2=0$. The inset shows the wave packets produced by interference of two wave packets on the $A\ ^1\Sigma^+$ state excited by first two 4 fs Gaussian pulses separated by delay times $\tau_1=1000$ a.u. ~ 24 fs (wp1) (solid) and $\tau_1=2000$ a.u. ~ 48 fs (wp2) (dashed).

There is a possibility for deexcitation of the first wave packet back to the ground electronic state by the second pulse. Using a 4 fs Gaussian pulse identical (in shape, width and carrier frequency) to the first pulse, we have calculated the deexcitation cross section to the ground state. It was found that at $\tau_1=1000$ a.u. deexcitation cross section is zero (not shown), whereas it is very high for $\tau_1=2000$ a.u. For deexcitation (at $\tau_1=2000$ a.u.), we have considered three resonant transitions from $v'=10$ of $A\ ^1\Sigma^+$ state to $v''=0\rightarrow 2$ of the ground state. Actually we have calculated the deexcitation cross section with three resonant frequencies ($v'=10 \rightarrow v''=0,1,2$) as the carrier frequencies to show that the deexcitation cross section to the ground vibrational level is maximum for $\tau_1=2000$ a.u. Although the central frequencies of the first and the second pulses are the same, due to the finite bandwidth of the two pulses, there is a finite probability that the higher vibrational levels of the ground state will be populated. Here the energy differences corresponding to $v'=10$ to $v''=0-2$ transitions are covered by the bandwidth. It can be shown that the cross sections for transitions from

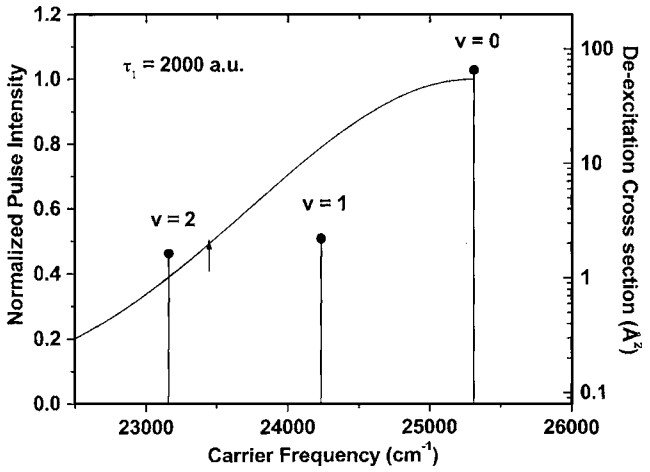

FIG. 3. Cross section for deexcitation of wave packet excited by a 4 fs Gaussian pulse (and evolved for $\tau_1=2000$ a.u.) on the $A\ ^1\Sigma^+$ state to different vibrational levels $v''=0$ to 2 of the ground $X\ ^1\Sigma^+$ state in NaH corresponds to the right vertical axis. The pulse used for deexcitation is a 4 fs Gaussian pulse with different carrier frequencies that correspond to deexcitation to different vibrational levels ($v''=0-2$) of the ground state. Half-intensity profile of the 4 fs Gaussian deexciting pulse is shown by the solid curve. The profile has been normalized to make the peak intensity value 1 and the normalized intensity has been plotted on the left vertical axis. The vertical arrow denotes half width of the Gaussian pulse.

higher vibrational levels, say $v'=11-14$ of the $A\ ^1\Sigma^+$ state to different vibrational levels $v''=0-4$, is negligible. Therefore we have shown in Fig. 3 the results for deexcitation to $v''=0-2$ levels of the ground state from $v'=10$ level of $A\ ^1\Sigma^+$ state which is possible due to finite bandwidth of the pulses. In Fig. 3, we have also plotted the half-intensity profile of the second 4 fs Gaussian pulse. The intensity profile has been normalized to obtain unit intensity at the peak. It is found that although the $v=1$ level is well within the half-width and $v=2$ level is very close to the half width, the contribution to $v=1$ and $v=2$ is almost two orders of magnitude smaller than that to $v=0$. Thus by controlling the delay τ_1 between the first two pulses, one can control the dissociation to the repulsive $B\ ^1\Pi$ state as well as the deexcitation to the $v''=0$ level of the ground state. At $\tau_1=2000$ a.u., we have got larger deexcitation cross section and smaller dissociation cross section as compared to those for $\tau_1=1000$ a.u. This is reflected in the position and magnitude of the interfering wave packet wp2 (inset of Fig. 2). For wp2 first two wave packets on the $A\ ^1\Sigma^+$ state interfere almost destructively reducing the magnitude of the resultant wave packet as because most of the population on this state is being deexcited back to the ground state by the second pulse. Similarly, at $\tau_1=1000$ a.u. (wp1 in inset of Fig. 2), we have got large dissociation and zero deexcitation cross section. The wave packets at this delay are interfering almost constructively to enhance the magnitude of the wave packet wp1 on the $A\ ^1\Sigma^+$ state and most of the population is being excited to the repulsive state. The probability for deexcitation of the wave packet wp1 and wp2 on the $A\ ^1\Sigma^+$ state by the third pulse is negligible as the frequency of the third pulse is much smaller than the first two pulses in spite of the finite bandwidth of the third pulse. This has been shown and discussed in the earlier work [23]. If the Rabi period of the pump pulse is smaller than its time duration, the wave packets formed on the excited state by the pump pulse should have a finite probability of being deexcited by the pump pulse itself. This could happen only for highly intense laser with very small Rabi period. In this case, we have found that the required intensity of the pulse for the Rabi period to be comparable to the pulse duration is $\sim 10^{12}$ Watt/cm^2. Hence one can neglect the dumping of population to the ground state by the first pulse, if the laser intensity is kept below 10^{12} Watt/cm^2.

The wave packets wp1 and wp2 shown in Fig. 2 at $\tau_2=0$ are propagated freely on the $A\ ^1\Sigma^+$ state for a finite time τ_2 to get wave packets ready for the excitation to the repulsive state by the third pulse. Two different excitation schemes (1) δ-function excitation and (2) excitation by 4 fs Gaussian pulse have been considered for the dissociation by the third pulse.

Here we have theoretically studied δ-function excitations to explore the dependence of dissociation cross section on the pulse shape and duration, although the generation of δ-function pulse is difficult in practice [46]. Recently, attosecond pulses are being used to study electronic motion in atoms [32]. In a previous calculation [23], we have also shown that a 1 femtosecond pulse can be approximated as δ-function pulse since the dissociation spectra obtained due to excitation by δ-function and 1 femtosecond pulses were almost the same.

In different studies on relativistic heavy ion collisions, the electromagnetic interaction of ultrarelativistic heavy ions was approximated as δ-function interaction. This approximation was found to be valid under conditions of high energy impact which does not involve too large energy transfer [47,48].

A. δ-function excitation

For the dissociation by the δ-function third pulse we have calculated the dissociation spectrum (i.e., cross section as a function of photon energy) for different values of τ_2 at two values of τ_1 by the Fourier transformation of autocorrelation function [see Eq. (3)]. The spectra for $\tau_2=0$ at two values of τ_1 have been shown in Fig. 2. Since the shape and the position of the wave packet on $A\ ^1\Sigma^+$ state (which is being excited by the δ-function pulse to the dissociative state) are different at different values of τ_1 and τ_2 and hence the dissociation spectra will also be different at different values of τ_1 and τ_2. From these spectra we have extracted the dissociation cross sections as a function of τ_2 at different values of photon energy and at two values of τ_1. In Figs. 4 and 5 dissociation cross sections as a function of τ_2 for two values of photon energies of the third pulse have been plotted at two different values of τ_1 as mentioned above. Figure 2 shows that the spectra cover a broad range of photon energies each of which will give rise to different spectra of dissociation fragments.

We have shown here the dissociation spectrum through the continuum of $B\ ^1\Pi$ state which leads to product states Na($2p$) and H($2s$). Dissociation spectrum shows appreciable

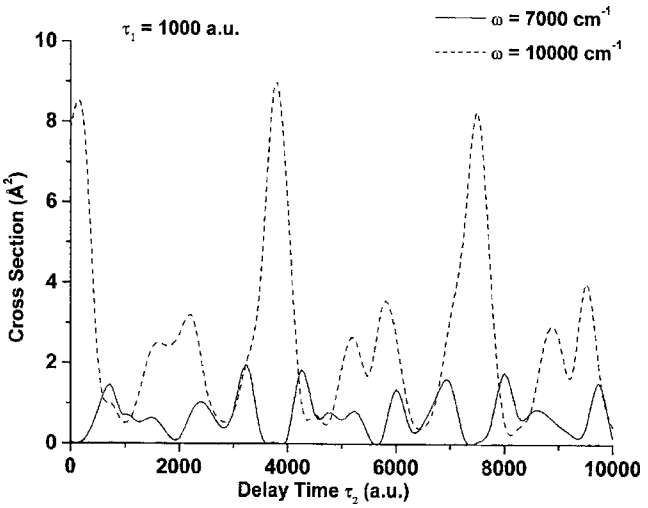

FIG. 4. Photodissociation cross section for δ-function excitation of the wave packet wp1 on the $A\ ^1\Sigma^+$ state (corresponding to $\tau_1=1000$ a.u.) at different delay times τ_2 between the second and the third pulses and at different photon energies $\omega=7000\ \mathrm{cm}^{-1}$ (solid curve) and $\omega=10\,000\ \mathrm{cm}^{-1}$ (dashed curve). In this figure and the following figures, the delay times have been presented in atomic units. To find the delay time in femtoseconds, one should multiply by 2.42×10^{-2}.

contribution in the range of photon energy $7500\ \mathrm{cm}^{-1}$ to $12\,500\ \mathrm{cm}^{-1}$. The next allowed electronic state is $C\ ^1\Sigma^+$ state which leads to product state $\mathrm{Na}(3p)+\mathrm{H}(2s)$. But the difference in continua of $B\ ^1\Pi$ and $C\ ^1\Sigma^+$ states is $8612\ \mathrm{cm}^{-1}$ [49]. Hence to excite continuum of $C^1\Sigma^+$ state the photon energy should be greater than $14\,600\ \mathrm{cm}^{-1}$. To excite continua of higher electronic states much larger photon energy than this is required. But different photon energies can lead to photofragments with same excess energy from continua of different electronic states. This excess energy will be shared by the photofragments in inverse mass ratio. Since continua of different states will lead to photofragments in different atomic states [e.g., $\mathrm{Na}(2p)$ for $B\ ^1\Pi$ state and $\mathrm{Na}(3p)$ for $C\ ^1\Sigma^+$ states] one will have to study energy spectrum of state selected atomic photofragments to determine the photon energy by which it is excited. State selection of photofragments can be done by different techniques like laser induced fluorescence, multiphoton ionization, etc. [50]. Therefore the dissociation cross sections at different values of photon energies covered by the bandwidth of the δ-function pulse can be realized in practice.

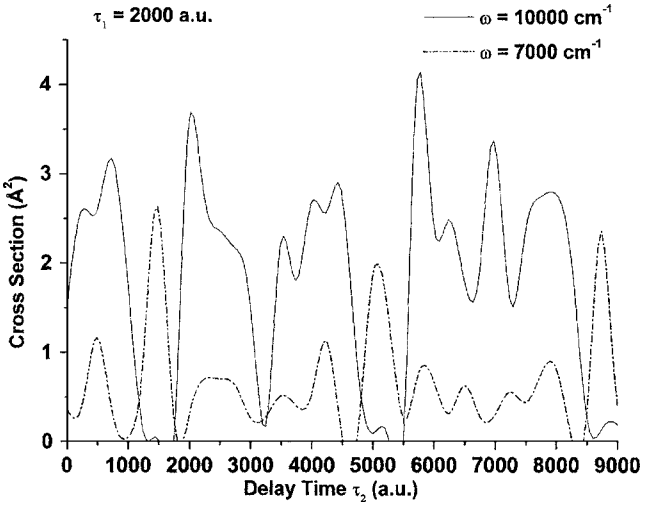

FIG. 5. Photodissociation cross section for δ-function excitation of the wave packet wp2 (corresponding to $\tau_1=2000$ a.u.) at different delay times τ_2 between the second and the third pulses and at different photon energies $\omega=7000\ \mathrm{cm}^{-1}$ (solid curve) and $\omega=10\,000\ \mathrm{cm}^{-1}$ (dashed curve).

For the δ-function excitation, the dissociation cross sections at different delay times τ_2 corresponding to $\tau_1=1000$ a.u. have been shown in Fig. 4 for two different photon energies $\omega=7000\ \mathrm{cm}^{-1}$ and $\omega=10\,000\ \mathrm{cm}^{-1}$. For both the photon energies, the cross section oscillates with the delay time, but the nature of oscillation is different for two energies. For these two energies, positions of minima and maxima of oscillations occur at different delay times (τ_2). This oscillation in the cross section can be used as time-dependent quantum gates [23]. For the chosen photon energies, the maxima and minima of the cross section are also different in magnitude. For $\omega=7000\ \mathrm{cm}^{-1}$, minima of the cross section are located at delays $\tau_2=0, 1000, 3700, 7500$ a.u. and maxima are at $\tau_2=3000, 4000, 7000, 8000$ a.u., etc., whereas the maxima and minima for $\omega=10\,000\ \mathrm{cm}^{-1}$ are located at 200, 3800, 7400 a.u. and 1000, 2800, 4600, 6200, and 8200 a.u., respectively. This demonstrates the dependence of the time-dependent gate on the photon energy covered by the bandwidth of the third pulse. Similar oscillation in cross section with delay can be seen for the wave packet wp2 (corresponding to $\tau_1=2000$ a.u.) as shown in Fig. 5. Comparing Figs. 4 and 5, one can find that the position and magnitude of minima and maxima of the cross section also depends on τ_1. This difference in the position of the maxima and the minima and their magnitudes are due to the difference in the location, shape, and magnitude of the two wave packets (wp1 and wp2). The cross section vs delay time graph in Fig. 5 has complex structure which reflects the complex shape of the initial wave packet wp2 on the $A^1\Sigma^+$ state. Moreover, the peaks and the zeros in the cross section are broad and are not so distinctive in nature as those in Fig. 4. This shows that time-dependent gates can be realized properly only for localized wave packets, which can be generated and controlled by very short pulses [23].

Due to the infinite bandwidth of the δ-function pulse there is a possibility that the molecule will be deexcited to the ground state by the third pulse. From the spectra shown in Fig. 2, it is clear that maximum of the dissociation occurs around the photon energies $9500\ \mathrm{cm}^{-1}$ and the energy spread around this photon energy is approximately $4500\ \mathrm{cm}^{-1}$. But the energy difference of the $v'=10$ level of $A\ ^1\Sigma^+$ state from the dissociation threshold of the ground state is approximately $11\,000\ \mathrm{cm}^{-1}$. The deexcitation by the third pulse within the energy range $7500\ \mathrm{cm}^{-1}$ to $12\,500\ \mathrm{cm}^{-1}$ for which dissociation cross section is prominent, deexcitation to lower vibrational levels will not be important [23,45]. However, due to infinite bandwidth of the δ-function pulse, all the lower vibrational levels of the ground state can be accessed

with photon energy higher than 11000 cm^{-1}. Let us consider deexcitation to different vibrational levels of the ground state by the δ-function third pulse. The probability of deexcitation to the ground state will be controlled by two factors (i) photon energy of the deexcitation pulse and (ii) Franck-Condon factors of different vibrational levels of the ground state with the wave packet on the $A^1\Sigma^+$ potential surface. In the previous section we have shown that although different lower vibrational levels ($v=0$, 1, and 2) are well within or close to the bandwidth of 4 fs pulse deexcitation occurs mainly to $v=0$ level. This is because of the fact that Franck-Condon factor for $v=0$ level dominates over other lower vibrational levels. Therefore one can control the Franck-Condon overlaps with different vibrational levels of the ground state by controlling the shape and position of the wave packet on the $A^1\Sigma^+$ state which is caused by the delay between two pulses. We have shown elsewhere [51] that the population distribution in different vibrational levels of the ground state can be controlled by the delay between excitation and deexcitation 4 fs pulses. In Figs. 4 and 5 we have given dissociation cross section for two different values of delay time, $\tau_1=1000$ a.u. and 2000 a.u., respectively. Therefore, for each value of τ_1, one will have to calculate deexcitation cross section to different vibrational levels of the ground state for different values of τ_2. For the present calculation we have not considered the effect of deexcitation from the $A^1\Sigma^+$ to the vibrational levels of the ground state by the third pulse. It will be interesting to study the deexcitation probability by the δ-function third pulse to different vibrational levels of the ground state which will depend both on the values of τ_1 and τ_2.

B. Excitation by 4 fs Gaussian pulse

When the wave packets wp1 and wp2 are excited to the $B\,^1\Pi$ state surface by a 4 fs Gaussian pulse, the photodissociation spectrum differs from that obtained for a δ-function transition [23]. The cross section for excitation of the wave packet wp1 at three different carrier frequencies have been plotted against the time delay τ_2 (Fig. 6). For all the three carrier frequencies, the cross section oscillates with delay time τ_2. For $\omega=7000$ cm^{-1} and 8000 cm^{-1}, the maxima and minima in the cross section values are located at the same delays. For $\omega=10\,000$ cm^{-1}, these are slightly shifted (by $\Delta\tau_2=500$ a.u. ~ 12 fs). The magnitude of cross section is different at the three carrier frequencies. The recurrence of the maxima and minima in the cross section for excitation by a 4 fs Gaussian pulse (Fig. 6) occurs more frequently as compared to that for the δ-function transition. This is because of the formation of delocalized wave packet by the finite pulse width on the repulsive state surface. The oscillation of the cross section with delay time is not as pronounced as that for a δ-function pulse. At very high delay time the oscillation is further damped due to spreading of the wave packet.

When the wave packet wp2 is excited to the repulsive surface, the spectrum is different in magnitude and shape from that for excitation of wp1. The cross section for excitation of the two wave packets wp1 and wp2 at different delay times τ_2 of the third pulse at carrier frequency $\omega=10\,000$ cm^{-1} have been compared in Fig. 7. As in the case

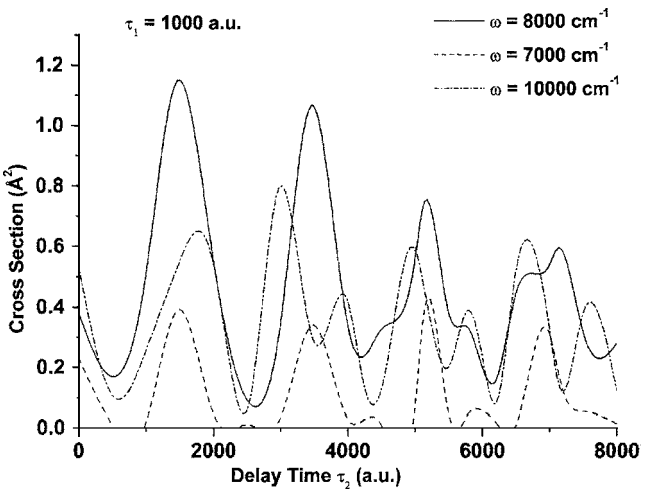

FIG. 6. Photodissociation cross section as a function of τ_2, for excitation by a 4 fs Gaussian pulse at different carrier frequencies $\omega=8000$ cm^{-1} (solid curve), $\omega=7000$ cm^{-1} (dashed curve), and $\omega=10\,000$ cm^{-1} (dashed-dotted curve) for $\tau_1=1000$ a.u.

of δ-function transition, the position of the maxima and minima are slightly shifted for the two wave packets. But in contrast to the δ-function excitation, the magnitude of cross section at the maxima for the two wave packets is comparable (for δ-function transition, the value of cross section at the maxima for the wave packet wp1 is almost twice as that for the wave packet wp2). The weak dependence of the magnitude of cross section at the maxima on τ_1 for excitation by 4 fs pulse is due to the delocalization of wave packets caused by the finite pulse duration. However, at these two delays ($\tau_1=1000$ a.u. and 2000 a.u.), the nature of oscillation of cross section with τ_2 is significantly different.

The wave packet oscillates on the $A^1\Sigma^+$ state between the inner and outer turning points. When the wave packet is excited by the third pulse to the repulsive state within the Franck-Condon region of the $v'=10$ level, the photodissocia-

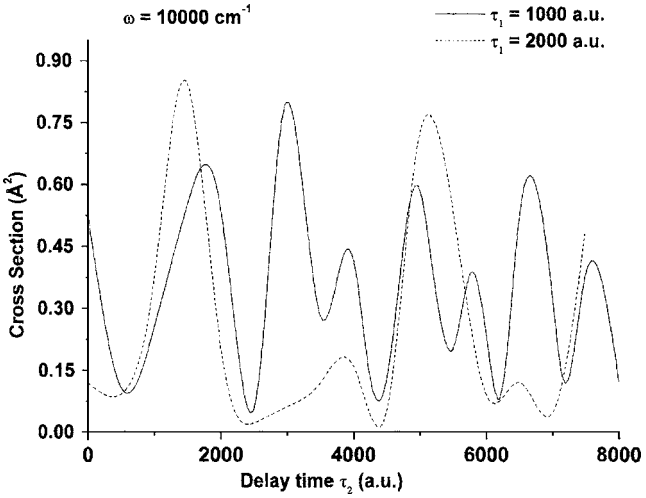

FIG. 7. Photodissociation cross section at different delay times τ_2 for excitation of wave packets corresponding to $\tau_1=1000$ a.u. (solid curve) and $\tau_1=2000$ a.u. (dashed curve) by a 4 fs Gaussian pulse at carrier frequency $\omega=10\,000$ cm^{-1}.

tion cross section will be high, whereas if the wave packet is excited away from the Franck-Condon region, cross section will be low. When the wave packet is localized, the period of oscillation is 3650 a.u. However, in this calculation, wave packets are delocalized on the $A^1\Sigma^+$ state due to the delay given between the two pulses. Hence the oscillation in dissociation cross section with time delay between the second and the third pulses is complex and the oscillation period is different from that in the case of localized wave packets [23]. We have studied the oscillation of this interferring wave packet on the $A^1\Sigma^+$ state. Due to space restriction, this dynamics of the wave packet has not been shown here; we have shown the wave packet only at two different delay times τ_1 as mentioned above. The dynamics of wave packet oscillation has been shown in a previous calculation [23].

V. CONCLUSION

The (1+1+1′)-photon dissociation cross section can be controlled by controlling the delays τ_1 and τ_2 between the three consecutive ultrashort pulses. A wave packet can be designed on the intermediate state by controlling the delay τ_1 between the first two pulses. This designed wave packet can be excited to the dissociative state by a third pulse whose delay τ_2 can be controlled to achieve control over the final dissociation cross section. The dissociation cross section also depends on the shape and duration of the pulse used for the third excitation, viz., δ-function and 4 fs Gaussian pulse. For both the transitions (by δ-function or 4 fs Gaussian pulses) the (1+1+1′)-photon dissociation cross section oscillates with delay time τ_2 between the second and the third pulse. The nature of this oscillation depends on the photon energy (covered by the bandwidth of δ-function pulses), on the carrier frequency (for 4 fs Gaussian pulses) and also on the delay between first two pulses. This oscillation in the cross section can be utilized as quantum gates. Furthermore, deexcitation cross section to the ground state by the second pulse can be controlled by the delay (τ_1) between first two pulses.

ACKNOWLEDGMENT

This work was done under financial support from BRNS, Department of Atomic Energy, Government of India.

[1] W. S. Warren, H. Rabitz, and M. Dahleh, Science **259**, 1581 (1993) and references therein.
[2] P. Brumer and M. Shapiro, Chem. Phys. Lett. **126**, 541 (1986); M. Shapiro and P. Brumer, J. Chem. Phys. **84**, 4103 (1986).
[3] A. P. Peirce, M. A. Dahleh, and H. Rabitz, Phys. Rev. A **37**, 4950 (1988).
[4] D. J. Tannor and S. A. Rice, J. Chem. Phys. **83**, 5013 (1985); D. J. Tannor, R. Kosloff, and S. A. Rice, J. Chem. Phys. **85**, 5805 (1986); S. A. Rice, Science **258**, 412 (1992); D. J. Tannor and S. A. Rice, Adv. Chem. Phys. **70**, 441 (1988); R. Stolow, Philos. Trans. R. Soc. London, Ser. A **356**, 345 (1998).
[5] M. Dantus, M. J. Rosker, and A. H. Zewail, J. Chem. Phys. **87**, 2395 (1987); T. S. Rose, M. J. Rosker, and A. H. Zewail, J. Chem. Phys. **88**, 6672 (1988).
[6] A. Lindinger, C. Lupulescu, M. Plewicki, F. Vetter, A. Merli, S. M. Weber, and L. Woste, Phys. Rev. Lett. **93**, 033001 (2004).
[7] H. Niikura, D. M. Villeneuve, and P. B. Corkum, Phys. Rev. Lett. **92**, 133002 (2004).
[8] T. Baumert, M. Grosser, R. Thalweiser, and G. Gerber, Phys. Rev. Lett. **67**, 3753 (1991); T. Brixner, N. H. Damrauer, and G. Gerber, Adv. At., Mol., Opt. Phys. **46**, 1 (2001).
[9] J. M. Papanikolas *et al.*, J. Chem. Phys. **103**, 7269 (1995).
[10] G. Alber, H. Ritsch, and P. Zoller, Phys. Rev. A **34**, 1058 (1986).
[11] P. Kowalczyk, C. Radzewicz, J. Mostowski, and I. A. Walmsley, Phys. Rev. A **42**, 5622 (1990).
[12] M. Lein, M. Erdmann, and V. Engel, J. Chem. Phys. **113**, 3609 (2000).
[13] S. Chelkowski, A. D. Bandrauk, and P. B. Corkum, Phys. Rev. Lett. **65**, 2355 (1990).
[14] N. Dudovich, B. Dayan, S. M. Gallagher Faeder, and Y. Silberberg, Phys. Rev. Lett. **86**, 47 (2001).
[15] R. S. Minns, R. Patel, J. R. R. Verlet, and H. H. Fielding, Phys. Rev. Lett. **91**, 243601 (2003).
[16] R. Uberna *et al.*, Faraday Discuss. **113**, 385 (1999).
[17] I. Walmsley and E. Rabitz, Phys. Today **56**(8), 43 (2003).
[18] M. W. Noel and C. R. Stroud, Jr., Phys. Rev. Lett. **75**, 1252 (1995).
[19] X. Chen and J. A. Yeazell, Phys. Rev. A **55**, 3264 (1997).
[20] V. Blanchet, M. A. Bouchene, and B. Girard, J. Chem. Phys. **108**, 4862 (1998).
[21] E. Skovsen, M. Machholm, T. Ejdrup, J. Thogersen, and H. Stapelfeldt, Phys. Rev. Lett. **89**, 133004 (2002).
[22] K. Ohmori, Y. Sato, E. E. Nikitin, and S. A. Rice, Phys. Rev. Lett. **91**, 243003 (2003).
[23] Anindita Bhattacharjee and Krishna Rai Dastidar, J. Phys. B **36**, 4467 (2003).
[24] A. Barenco, D. Deutsch, A. Ekert, and R. Jozsa, Phys. Rev. Lett. **74**, 4083 (1995).
[25] R. Pausch, M. Heid, T. Chen, W. Kiefer, and H. Schwoerer, J. Chem. Phys. **110**, 9560 (1999).
[26] G. G. Balint-Kurti, R. N. Dixon, and C. C. Marston, Int. Rev. Phys. Chem. **11**, 317 (1992) and references therein.
[27] P. M. Regan, D. Ascenzi, A. Brown, G. G. Balint-Kurti, and A. J. Orr-Ewing, J. Chem. Phys. **112**, 10259 (2000); A. Brown and G. G. Balint-Kurti, *ibid.* **113**, 1879 (2000).
[28] A. Bhattacharjee and K. R. Dastidar, Phys. Rev. A **65**, 022701 (2002); A. Bhattacharjee and K. Rai Dastidar, Pramana **58**, 569 (2002).
[29] E. J. Heller, J. Chem. Phys. **68**, 2066 (1978).
[30] S. Y. Lee and E. J. Heller, J. Chem. Phys. **71**, 4777 (1979).
[31] A. Baltuska *et al.*, *Femtosecond Optical Frequency Comb Technology*, edited by J. Ye and S. T. Cundiff (Springer, New York, 2005), p. 263; P. M. Paul *et al.*, Science **292**, 1689

(2001); M. Drescher *et al.*, Science **291**, 1923 (2001); P. Antoine, A. L'Huillier, and M. Lewenstein, Phys. Rev. Lett. **77**, 1234 (1996); G. Steinmeyer *et al.*, Science **286**, 1507 (1999).
[32] M. Hentschel *et al.*, Nature (London) **414**, 509 (2001); M. Drescher *et al.*, Nature (London) **419**, 803 (2002).
[33] A. Baltuska *et al.*, Nature (London) **421**, 611 (2003); R. Kienberger *et al.*, Science **297**, 1144 (2002).
[34] A. D. Bandrauk and N. H. Shon, Phys. Rev. A **66**, 031401(R) (2002); E. Eremina, X. Liu, H. Rottke, W. Sandner, M. G. Schatzel, A. Dreischuh, G. G. Paulus, H. Walther, R. Moshammer, and J. Ullrich, Phys. Rev. Lett. **92**, 173001 (2004).
[35] C. C. Marston and G. G. Balint-Kurti, J. Chem. Phys. **91**, 3571 (1989).
[36] R. Kosloff, J. Phys. Chem. **92**, 2087 (1988).
[37] V. Engel, R. Schinke, S. Hennig, and H. Metiu, J. Chem. Phys. **92**, 1 (1990); R. Schinke, *Photodissociation Dynamics* (Cambridge University Press, Cambridge, UK, 1993).
[38] W. T. Pollard, S. Y. Lee, and R. A. Mathies, J. Chem. Phys. **92**, 4012 (1990).
[39] X. Liu *et al.*, Phys. Rev. Lett. **93**, 263001 (2004).
[40] S. T. Cundiff, J. Phys. D **35**, R43 (2002); L. Xu, C. Spielmann, A. Poppe, T. Brabec, F. Krausz, and T. W. Hansch, Opt. Lett. **21**, 2008 (1996).
[41] T. Brabec and F. Krausz, Rev. Mod. Phys. **72**, 545 (2000).
[42] Z. Zeng *et al.*, Phys. Rev. A **67**, 013815 (2003); I. P. Christov *et al.*, Opt. Express **7**, 362 (2000); G. Tempea, M. Geissler, and T. Brabec, J. Opt. Soc. Am. B **16**, 669 (1999).
[43] S. Chelkowski and A. D. Bandrauk, Phys. Rev. A **65**, 061802(R) (2002); A. D. Bandrauk, S. Chelkowski, and N. H. Shon, Phys. Rev. A **68**, 041802(R) (2003).
[44] D. B. Milosevic, G. G. Paulus, and W. Becker, Phys. Rev. A **71**, 061404(R) (2005); G. G. Paulus, F. Lindner, H. Walther, A. Baltuska, E. Goulielmakis, M. Lezius, and F. Krausz, Phys. Rev. Lett. **91**, 253004 (2003); D. B. Milosevic, G. G. Paulus, and W. Becker, Laser Phys. Lett. **1**, 93 (2004); G. G. Paulus *et al.*, Nature (London) **414**, 182 (2001); P. Dietrich *et al.*, Opt. Lett. **25**, 16 (2000); D. B. Milosevic *et al.*, Opt. Express **11**, 1418 (2003); E. Cormier and P. Lambropoulos, Eur. Phys. J. D **2**, 15 (1998).
[45] E. S. Sachs, J. Hinze, and N. H. Sabelli, J. Chem. Phys. **62**, 3367 (1975); **62**, 3384 (1975).
[46] W. H. Knox, R. S. Knox, J. F. Hoose, and R. N. Zare, Opt. Photonics News **1**, 44 (1990).
[47] C. A. Bertulani, nucl-th/0012038v2.
[48] A. J. Baltz, Phys. Rev. A **52**, 4970 (1995) and references therein.
[49] W. C. Stwalley, W. T. Zemke, and S. C. Yang, J. Phys. Chem. Ref. Data **20**, 153 (1991) and references therein.
[50] R. J. Van Brunt and R. N. Zare, J. Chem. Phys. **48**, 4304 (1968); C. H. Greene and R. N. Zare, *ibid.* **78**, 6741 (1983); T. P. Rakitzis, S. A. Kandel, and R. N. Zare, *ibid.* **108**, 8291 (1998).
[51] A. Bhattacharjee and K. Rai Dastidar (private communication).